Mathematical Modeling of the Steady-State Behavior of Nitric Oxide in Brain

Corina S. Drapaca and Andrew Tamis

Abstract Nitric oxide (NO) is a small diffusible molecule that plays an important role in brain's signalling processes and regulation of cerebral blood flow and pressure. While most of the NO production is achieved through various chemical reactions taking place in the neurons, endothelial cells, and red blood cells, only the endothelial NO is activated by the shear stress at the blood-endothelium interface. NO is removed from the brain by blood's hemoglobin and through diffusion and other chemical processes. Given its relevance to brain functions, numerous studies on NO exist in the literature. The majority of the mathematical models of NO biotransport are diffusion-reaction equations predicting the spatio-temporal distribution of NO concentration either inside or outside the blood vessels, and do not account for the endothelial NO production through mechanotrasduction. In this paper we propose a mathematical model of the steady-state behavior of NO in the brain that links the NO synthesis and inactivation from inside and outside a cerebral arteriole and the blood flow. The blood flow is assumed to be a Poiseuille flow, and we use two models of blood: viscous Newtonian and non-local non-Newtonian fluids. The model is used to study through numerical simulations the effects of the cerebral blood pressure on the NO concentration.

Keywords Cerebral Nitric Oxide · Poiseuille Flow · Mechanotransduction · Fractional Calculus · Nonlocality

1 Introduction

Nitric oxide (NO) is a free radical gas involved in many critical bio-chemical processes taking place in living organisms. In particular, NO acts as a neuro-glial-vascular messager and regulator of cerebral blood flow [1, 2, 6, 7, 10, 11, 14,

C. S. Drapaca (✉) · A. Tamis
Pennsylvania State University, State College, University Park, PA 16802, USA
e-mail: csd12@psu.edu

A. Tamis
e-mail: apt5288@psu.edu

D. M. Kilgour et al. (eds.), *Recent Developments in Mathematical, Statistical and Computational Sciences*, Springer Proceedings in Mathematics & Statistics 343,
https://doi.org/10.1007/978-3-030-63591-6_47

15, 18, 20–22]. NO is produced by synthesis reactions taking place in specific neurons [10], vascular endothelium and choroid plexus [11], and red blood cells [15]. While neuronal NO is involved in learning, memory formation, and regulation of the cerebral blood flow [11], the endothelial NO maintains cerebral microcirculation by guiding vasomotor responses and vasoprotection processes, and by reducing the cerebral blood pressure [1, 10, 12, 13]. The endothelial NO can also be produced through mechanotransduction initiated by the shear stress at the endothelium-blood interface [25]. The NO formed in the deoxygenated red blood cells is involved in the red blood cells deformability [3]. NO is removed from the brain by blood's hemoglobin and through diffusion and other chemical processes [15].

Given the essential role played by NO in various physiological and pathophysiological processes, especially those involved in brain functions, numerous mathematical models of NO spatio-temporal dynamics exist in the literature [5, 14, 16, 26, 27] (a comprehensive review of mathematical models of NO biotransport is given in [5]). The majority of these models are reaction-diffusion equations describing NO syntheses (production) and inactivation (loss) either inside or outside the blood vessels. The shear-induced production of the endothelial NO and the coupling of the NO contributions from the inside and outside of the blood vessels are usually modelled as known boundary conditions. Since these models do not incorporate any mechanical properties of cells and their interactions, they cannot accurately predict the NO effects on, for instance, cerebral blood flow and vasculature, and ultimately on brain fuctions. A mathematical model that couples the NO spatio-temporal dynamics and the mechanical behaviors of blood flow and vasculature could prove essential in the development of successful NO-based therapies for clinical conditions associated with disturbances in NO production and/or signaling [4].

In this paper we propose a mathematical model for the steady-state behavior of NO in brain that incorporates the production of endothelial NO through shear-induced mechanotransduction. The steady-state reaction-diffusion equation for the NO concentration includes production and decay terms from the inside and outside of a cerebral arteriole which are taken from [14, 16, 26, 27]. A new NO production term is added to the equation that models the shear-induced mechanotransduction of NO in endothelium. This production term is assumed to be proportional to the concentration of NO which is in agreement with the experimental observations reported in [25]. We further conjecture that the production rate of this term is proportional to the viscous dissipation at the blood flow-endothelium interface. Dissipation is calculated from assumptions on the mechanical properties of the blood flow and arteriolar wall. For now, the wall is assumed to be rigid and permeable only to NO. The blood flow is modelled as a Poiseuille flow, and we use two models of blood: viscous Newtonian and non-local non-Newtonian fluids. The non-Newtonian nature of blood becomes apparent in the smaller vessels such as the arterioles. Here we use the non-local non-Newtonian model of blood proposed in [8] which accounts for long-range chemo-mechanical interactions of the red blood cells in vivo. The model is used to study through numerical simulations the effects of the cerebral blood pressure on the NO concentration.

The paper is structured as follows. Section 2 presents the mathematical model, while the numerical results are shown in Sect. 3. The paper ends with conclusions and suggestions for future work.

2 Mathematical Model

The geometric domain shown in Fig. 1 is made of concentric horizontal axi-symmetric circular cylinders. The cylinders have rigid walls which are permeable only to NO. The blood flows through the lumen region of radius R. The endothelium layer of the arteriole has thickness h and is considered separately from the other arteriolar layers because it is a NO production site. The next region of thickness d is made of the other vascular layers and extracellular space. Lastly, the region of thickness g represents a group of neurons that produce NO.

As in [26, 27], the NO transport by convection is neglected. The blood is an incompressible fluid in a three-dimensional fully-developed steady laminar flow. The flow is axi-symmetric and driven by an externally applied pressure gradient. No body forces are acting on the blood. In cylindrical coordinates (r, θ, z), only the axial component of the blood's velocity is non-zero. Thus, at steady-state, the concentration of NO, c_{NO}, and the axial component of the blood's velocity, w, depend only on the independent variable r.

The NO is produced in the region $[R,\ R+h] \cup [R+h+d,\ R+h+d+g]$ and decays in the region $[0,\ R] \cup [R+h,\ R+h+d+g]$. In addition, NO diffuses radially on $[0,\ R+h+d+g]$. Thus, the balance law of mass at steady-state in cylindrical coordinates is:

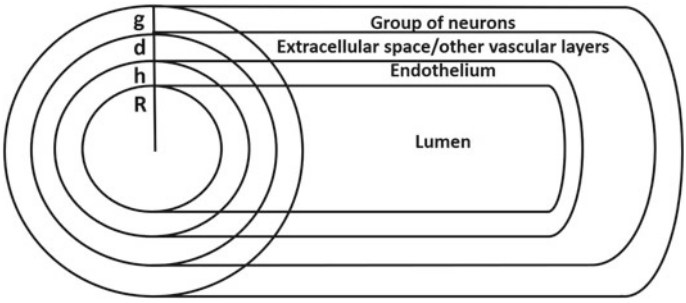

Fig. 1 The geometric domain is made of concentric horizontal axi-symmetric circular cylinders. The regions correspond to the lumen of radius R, endothelium of thickness h, a region of thickness d made of other arteriolar layers and extracellular space, and a region of thickness g filled with neurons

$$D_{NO}\left(\frac{d^2c_{NO}}{dr^2}+\frac{1}{r}\frac{dc_{NO}}{dr}\right)+\nu_1 H(r-(R+h+d))-\frac{V_{max}c_{NO}}{K_{max}+c_{NO}}H(r-(R+h))$$
$$+\frac{\sigma_{rz}}{\tau_w}\frac{dw}{dr}(H(r-R)-H(r-(R+h)))c_{NO}-\lambda(1-H(r-R))c_{NO}=0 \quad (1)$$

In Eq. (1), D_{NO} is the diffusion coefficient of NO, ν_1 is the constant rate of NO synthesis in the neurons, V_{max} is the maximum rate at saturating concentration of NO in the region $[R+h,\ R+h+d+g]$, and K_{max} is the NO concentration at which the reaction rate is $V_{max}/2$ in the region $[R+h,\ R+h+d+g]$ [14]. The viscous dissipation is the product between blood's shear stress σ_{rz} and $\frac{dw}{dr}$. The shear stress at the lumen-endothelium interface is $\tau_w=\sigma_{rz}(R)$. Lastly, the decay of NO due to the hemoglobin in blood is assumed to happen at a constant rate λ [16, 26, 27]. The Heaviside step function is denoted by H. The newly introduced fourth term in Eq. (1) is *the shear-induced production of NO in the endothelium*. Equation (1) was solved numerically and thus the presence of the discontinuous Heaviside step function in the equation did not pose any issues. In subsequent work a mathematical analysis of this equation with smooth coefficients will be performed to better understand the mathematical behavior of the solution and its physical interpretation.

The expressions for σ_{rz}, $\frac{dw}{dr}$, and τ_w are given further. The following assumptions specific to a Poiseuille flow in the region $[0,\ R]$ are made. Let $C=\dfrac{dp}{dz}<0$ be the constant, externally applied pressure gradient, where $p(z)$ is the hydrostatic pressure of blood. The lumen-endothelium interface is assumed to be a no slip boundary. The boundary condition at $r=0$ expresses the axial symmetry of the flow.

Newtonian Model of Blood For an incompressible viscous Newtonian fluid, the shear stress σ_{rz} and shear rate $\frac{dw}{dr}$ are related through the following constitutive relation:

$$\sigma_{rz}=\mu\frac{dw}{dr} \quad (2)$$

where μ is the dynamic viscosity. The solution of the Navier-Stokes equations at equilibrium with boundary conditions:

$$w(R)=\frac{dw}{dr}(0)=0 \quad (3)$$

is:

$$w(r)=\frac{C}{4\mu}\left(r^2-R^2\right) \quad (4)$$

Thus:

$$\frac{dw}{dr} = \frac{Cr}{2\mu},\ \sigma_{rz} = \frac{Cr}{2},\ \tau_w = \frac{CR}{2} \tag{5}$$

Since $C < 0$, a change of sign is required in front of the fourth term of equation (1) such that the term models NO production. Thus, by replacing formulas (5) in Eq. (1), Eq. (1) becomes:

$$D_{NO}\left(\frac{d^2c_{NO}}{dr^2} + \frac{1}{r}\frac{dc_{NO}}{dr}\right) + v_1 H(r-(R+h+d)) - \frac{V_{max}c_{NO}}{K_{max}+c_{NO}}H(r-(R+h)) \\ -\frac{Cr^2}{2\mu R}(H(r-R)-H(r-(R+h)))c_{NO} - \lambda(1-H(r-R))c_{NO} = 0 \tag{6}$$

Non-local Non-Newtonian Model of Blood The shear stress σ_{rz} for an incompressible non-local non-Newtonian fluid is given by [8]:

$$\sigma_{rz} = \mu\, D_r^{\alpha} w(r) \tag{7}$$

where $D_r^{\alpha} w(r)$ is the left-sided Caputo fractional derivative of order α which, by definition, is:

$$D_r^{\alpha} w(r) = \frac{1}{\Gamma(m-\alpha)}\int_0^r \frac{1}{(r-s)^{\alpha+1-m}}\frac{d^m w(s)}{ds^m}ds,\ m-1<\alpha<m$$

or

$$D_r^{\alpha} w(r) = \frac{d^m}{dr^m}w(r),\ \alpha = m$$

for $m \in \{1, 2, 3, ...\}$. From a physical point of view, $D_r^{\alpha} w(r)$ in formula (7) represents the shear rate of order α.

For $\alpha = 1$, formula (7) reduces to formula (2) and the physical parameter μ becomes the apparent viscosity. Parameter $\alpha \neq 1$ gives an intrinsic coupling between flow and the continuous rearrangement of the fluid's microstructure during flow. The information about this coupling is lost when $\alpha = 1$. Thus, the constitutive equation (7) for $\alpha \neq 1$ models long-range (non-local) interactions among cells caused by and contributing to blood flow in vivo.

The solution of the Navier-Stokes equations at equilibrium with the boundary conditions:

$$w(R) = \frac{d^k}{dr^k}w(0+) = 0,\ k = 1, 2, ..., m-1,\ m-1<\alpha<m \tag{8}$$

is [8]:

$$w(r) = \frac{C}{2\mu\alpha(\alpha+1)\Gamma(\alpha)}\left(r^{\alpha+1} - R^{\alpha+1}\right). \tag{9}$$

Thus:

$$\frac{dw}{dr} = \frac{Cr^{\alpha}}{2\mu\alpha\Gamma(\alpha)},\ \sigma_{rz} = \frac{Cr}{2},\ \tau_w = \frac{CR}{2} \tag{10}$$

Lastly, by replacing formulas (10) in Eq. (1) and using the same sign convention as before, the following equation is obtained for c_{NO}:

$$D_{NO}\left(\frac{d^2c_{NO}}{dr^2} + \frac{1}{r}\frac{dc_{NO}}{dr}\right) + \nu_1 H(r-(R+h+d)) - \frac{V_{max}c_{NO}}{K_{max}+c_{NO}}H(r-(R+h)) - \frac{Cr^{\alpha+1}}{2\mu R\alpha\Gamma(\alpha)}(H(r-R)-H(r-(R+h)))c_{NO} - \lambda(1-H(r-R))c_{NO} = 0 \tag{11}$$

If $\alpha = 1$, Eq. (11) reduces to Eq. (6). Thus, it suffices to build a numerical solution only for Eq. (11).

3 Results

The values of the parameters used in the numerical simulations are given in Table 1.

Two values for C are used which are named healthy and high. For the Newtonian model of blood, healthy and high pulse pressures in humans are estimated from [24]. For the non-local non-Newtonian model of blood, the healthy pressure gradient is

Table 1 List of parameters with corresponding values and units

Model of blood	Parameters	Values and units (Reference)
	R	25×10^{-6} m [16]
	h	0.5×10^{-6} m [16]
	d	4×10^{-6} m
	g	5×10^{-6} m [14]
	D_{NO}	3.3×10^{-9} m^2/s [14, 16]
	ν_1	1.6×10^{-3} mol/(m$^3 \times s$) [14]
	V_{max}	2×10^{-3} mol/(m$^3 \times s$) [14]
	K_{max}	10^{-6} mol/m^3 [14]
	λ	2.3×10^2 1/s [26]
Newtonian	μ	3 g/(m $\times$ s) [17]
	C (healthy)	-5.3×10^8 g/(m$^2 \times$ s^2) [24]
	C (high)	-7.9×10^8 g/(m$^2 \times$ s^2) [24]
Non-local Non-Newtonian	α	1.97 [9]
	μ	$0.021 \times 10^{6(\alpha-2)}$ g/(m$^{2-\alpha} \times$ s) [9]
	C (healthy)	-7.122×10^7 g/(m$^2 \times$ s^2) [9]
	C (high)	-7.122×10^{10} g/(m$^2 \times$ s^2)

estimated from experiments performed on a living mouse and reported in [19]. A high pressure gradient in living mice was not found in the literature and, therefore, this is chosen to be a value at which a difference in c_{NO} is observed from the healthy case. However, this high value of C might not be physiological. Lastly, parameters α and μ of the non-local non-Newtonian model were found in [9] by fitting the speed given in formula (9) to the blood speed measured in vivo in a venule of a mouse cremaster muscle before systemic hemodilution [19].

Equation (11) is solved numerically using a zero Neumann boundary condition at $r = 0$:

$$\frac{dc_{NO}}{dr}(0) = 0 \tag{12}$$

and the following Dirichlet boundary condition at $r = R + h + d + g$ estimated from [14]:

$$c_{NO}(R + h + d + g) = 10^{-8}\ [mol/m^3] \tag{13}$$

Numerical solutions are obtained using the built-in function **bvp5c** in MATLAB. The function **bvp5c** solves boundary-value problems for systems of first order ordinary differential equations using the four-stage Lobatto IIIA formula represented as an implicit Runge-Kutta formula [23]. The system of first order differential equations corresponding to Eq. (11) is:

$$\begin{aligned}
&\frac{dc_{NO}}{dr} = s_{NO},\\
&\frac{ds_{NO}}{dr} = -\frac{1}{r}s_{NO} - \frac{v_1}{D_{NO}}H(r-(R+h+d)) + \frac{V_{max}c_{NO}}{D_{NO}(K_{max}+c_{NO})}H(r-(R+h))\\
&+\frac{Cr^{\alpha+1}}{2D_{NO}\mu R\alpha\Gamma(\alpha)}(H(r-R)-H(r-(R+h)))c_{NO} + \frac{\lambda}{D_{NO}}(1-H(r-R))c_{NO}
\end{aligned} \tag{14}$$

Thus, the function **bvp5c** solves system (14) with boundary conditions (12)–(13) for the unknowns c_{NO} and s_{NO}.

The results are shown in Fig. 2. Both models of blood show similar profiles for c_{NO} for their respective healthy and high values of C.The profiles of c_{NO} inside and outside the arteriole agree with those found in the literature. However, in the endothelium region (Fig. 2c, d) the concentration of NO for the high value of C is slightly higher than the one corresponding to the healthy value of C. These findings suggest that the blood pressure could affect the concentration of NO. The concentration of NO is more sensitive to changes in C when using the Newtonian model of blood then when the blood is modeled as a non-local non-Newtonian fluid. Since the blood flowing through small arterioles is non-Newtonian, it is possible that the concentration of NO is not affected by higher values of the cerebral blood pressure which are within physiological limits. Nevertheless, given the uncertainties in the values of the parameters in Table 1 and the inconsistencies among these parameters (some parameters were estimated from slices of rat brains [14], others from cremaster muscles of mice [19], and the rest from humans [17, 24]), a careful sensitivity analysis needs to

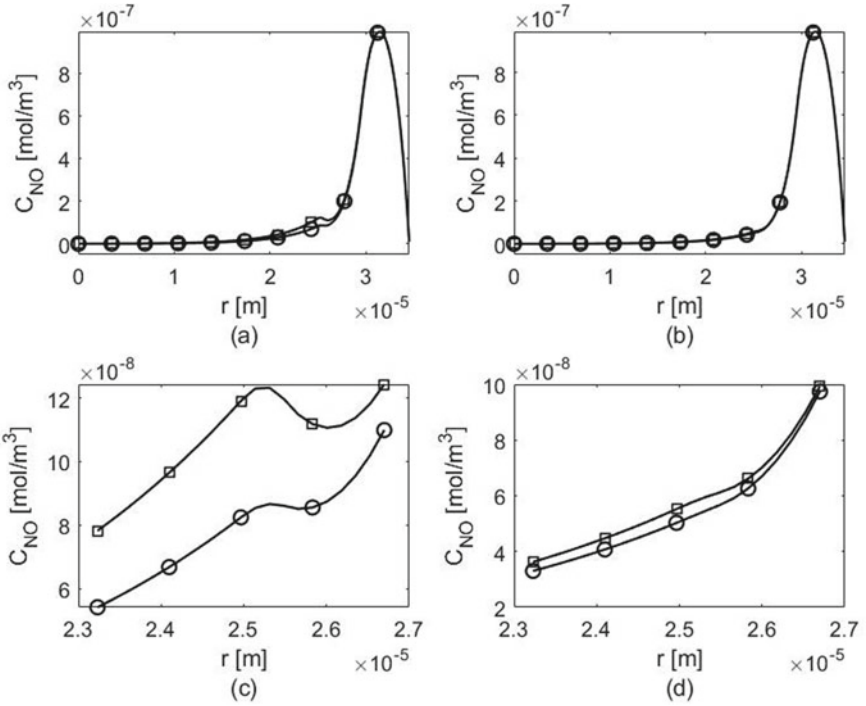

Fig. 2 Concentrations of NO for healthy (circle symbol) and high (square symbol) pressure gradients C: **a** Newtonian model of blood ($\alpha = 1$), **b** Non-local non-Newtonian model of blood ($\alpha = 1.97$). Zoom-ins of the plots (**a**) and (**b**) are shown in plots (**c**) and respectively (**d**). The region around the endothelium is chosen for the zoom-ins. c_{NO} in the endothelium is higher for a higher value of C, as expected from Eqs. (6) and (11)

be performed in order to get a better understanding of the relationship between the NO concentration and the cerebral blood flow and pressure and confirm the validity of these preliminary results.

4 Conclusion

In this paper, a mathematical model was proposed to describe the steady-state behavior of NO in brain. The model is a one-dimensional, steady-state reaction-diffusion equation for the concentration of NO that includes production and decay terms from the inside and outside of a cerebral arteriole which were taken from the literature. A new production term is added to the equation that models the NO production in the endothelium through shear-induced mechanotransduction. This production term is proportional to the concentration of NO and the corresponding production rate is

proportional to the viscous dissipation at the blood flow-endothelium interface. The dissipation was calculated using two mechanical models of blood: viscous Newtonian and non-local non-Newtonian fluids. The blood flow was a Poiseuille flow through an axi-symmetric circular cylinder whose wall was rigid and permeable only to NO. Numerical simulations suggest that the concentration of NO in the endothelium is higher at higher gradients of the cerebral blood pressure. This is a very promising result since it could help understand the effects of high blood pressure on the NO concentration. Incorporating the NO production by deoxygenated red blood cells and the viscoelasticity of the endothelium in the model and performing a sensitivity analysis of the model's parameters could provide more accurate predictions of the spatio-temporal distribution of the NO concentration in brain, and thus these will be the focus of future work.

References

1. Attwell, D., Buchan, A., Charpak, S., Lauritzen, M., MacVicar, B.A., Newman, E.A.: Glial and neuronal control of brain blood flow. Nature **468**, 232–243 (2010). https://doi.org/10.1038/nature09613
2. Barbosa, R.M., Lourenco, C.F., Santos, R.M., Pomerleau, F., Huettl, P., Gehardt, G.A., Laranjinha, J.: In vivo real-time measurement of nitric oxide in anesthetized rat brain. Methods Enzymol. **441**, 351–367 (2008). https://doi.org/10.1016/S0076-6879(08)01220-2
3. Bizjak, D.A., Brinkmann, C., Bloch, W., Grau, M.: Increase in red blood cell-nitric oxide synthase dependent nitric oxide production during red blood cell aging in health and disease: a study on age dependent changes of rheologic and enzymatic properties in red blood cells. PLoS ONE **10**(4) (2015). https://doi.org/10.1371/journal.pone.0125206
4. Bryan, N.S.: Nitric oxide enhancement strategies. Future Sci. OA. **1**(1), FSO48 (2015). https://doi.org/10.4155/FSO.15.48
5. Buerk, D.G.: Can we model nitric oxide biotransport? A survey of mathematical models for a simple diatomic molecule with surprisingly complex biological activities. Annu. Rev. Biomed. Eng. **3**, 109–143 (2001). https://doi.org/10.1146/annurev.bioeng.3.1.109
6. Buerk, D.G., Ances, B.M., Greenberg, J.H., Detre, J.A.: Temporal dynamics of brain tissue nitric oxide during functional forepaw stimulation in rats. NeuroImage **18**, 1–9 (2003)
7. Contestabile, A., Monti, B., Polazzi, E.: Neuronal-glial interactions define the role of nitric oxide in neural functional processes. Curr. Neuropharmacol. **10**(4), 303–310 (2012). https://doi.org/10.2174/157015912804143522
8. Drapaca, C.S.: Poiseuille flow of a non-Local non-Newtonian fluid with wall slip: a first step in modeling cerebral microaneurysms. Fractal. Fract. **2**(9) (2018). https://doi.org/10.3390/fractalfract2010009
9. Drapaca, C.S., Zhang, Z., Meng, R.: A comparison of constitutive models of blood (2018). arXiv:1808.07977
10. Forstermann, U., Sessa, W.C.: Nitric oxide synthases: regulation and function. Eur. Heart J. **33**, 829–837 (2012). https://doi.org/10.1093/eurheartj/ehr304
11. Garry, P.S., Ezra, M., Rowland, M.J., Westbrook, J., Pattinson, K.T.S.: The role of the nitric oxide pathway in brain injury and its treatment—from bench to bedside. Exp. Neurol. **263**, 235–243 (2015). https://doi.org/10.1016/j.expneurol.2014.10.017
12. Gordon, G.R.J., Mulligan, S.J., MacVicar, B.A.: Astrocyte control of the cerebrovasculature. Glia **55**, 1214–1221 (2007). https://doi.org/10.1002/glia.20543
13. Gordon, G.R., Howarth, C., MacVicar, B.A.: Bidirectional control of arteriole diameter by astrocytes. Exp. Physiol. **96**(4), 393–399 (2011). https://doi.org/10.1113/expphysiol.2010.053132

14. Hall, C.N., Garthwaite, J.: Inactivation of nitric oxide by rat cerebellar slices. J. Physiol. **577**(2), 549–567 (2006). https://doi.org/10.1113/jphysiol.2006.118380
15. Helms, C.C., Liu, X., Kim-Shapiro, D.B.: Recent insights into nitrite signaling processes in blood. Biol. Chem. **3**, 319–329 (2016). https://doi.org/10.1515/hsz-2016-0263
16. Kavdia, M., Tsoukias, N.M., Popel, A.S.: Model of nitric oxide diffusion in an arteriole: impact of hemoglobin-based blood substitute. Am. J. Physiol. Heart Circ. Physiol. **282**, H2245–H2253 (2002). https://doi.org/10.1152/ajpheart.00972.2001
17. Klabunde, R.E.: Cardiovascular physiology concepts (2017). https://www.cvphysiology.com/Hemodynamics/H011. Cited 11 Sept 2019
18. Ledo, A., Barbosa, R.M., Gerhardt, G.A., Cadenas, E., Laranjinha, J.: Concentration dynamics of nitric oxide in rat hippocampal subregions evoked by stimulation of the NMDA glutamate receptor. Proc. Natl. Acad. Sci. USA **102**(48), 17483–17488 (2005). https://doi.org/10.1073/pnas.0503624102
19. Long, D.S., Smith, M.L., Pries, A.R., Ley, K., Damiano, E.R.: Microviscometry reveals reduced blood viscosity and altered shear rate and shear stress profiles in microvessels after hemodilution. Proc. Natl. Acad. Sci. USA **101**(27), 10060–10065 (2004). https://doi.org/10.1073/pnas.0402937101
20. Mishra, A.: Binaural blood flow control by astrocytes: listening to synapses and the vasculature. J. Physiol. **595**(6), 1885–1902 (2017). https://doi.org/10.1113/JP270979
21. Moncada, S., Palmer, R.M.J., Higgs, E.A.: Nitric oxide: physiology, pathophysiology, and pharmacology. Pharmacol. Rev. **43**(2), 109–142 (1991)
22. Santos, R.M., Lourenco, C.F., Ledo, A., Barbosa, R.M., Laranjinha, J.: Nitric oxide inactivation mechanisms in the brain: role in bioenergetics and neurodegeneration. Int. J. Cell Biol. (2012). https://doi.org/10.1155/2012/391914
23. Shampine, L.F., Kierzenka, J.: A BVP solver that controls residual and error. J. Numer. Anal. Ind. Appl. Math. **3**(1–2), 27–41 (2008)
24. Sheps, S.G.: Pulse pressure: an indicator of heart health? (2019). https://www.mayoclinic.org/diseases-conditions/high-blood-pressure/expert-answers/pulse-pressure/faq-20058189. Cited 11 Sept 2019
25. Sriram, K., Laughlin, J.G., Rangamani, P., Tartakovsky, D.M.: Shear-induced nitric oxide production by endothelial cells. Biophys. J. **111**, 208–221 (2016). https://doi.org/10.1016/j.bpj.2016.05.034
26. Vaughn, M.W., Kuo, L., Liao, J.C.: Effective diffusion distance of nitric oxide in the microcirculation. Vasc. Physiol. **274**(5), H1705–H1714 (1998). https://doi.org/10.1152/ajpheart.1998.274.5.H1705
27. Vaughn, M.W., Kuo, L., Liao, J.C.: Estimation of nitric oxide production and reaction rates in tissue by use of a mathematical model. Am. J. Physiol. **274**(6), H2163–H2176 (1998). https://doi.org/10.1152/ajpheart.1998.274.6.H2163